Journal of Bioscience and Bioengineering
VOL. 127 No. 2, 246–255, 2019

www.elsevier.com/locate/jbiosc

Anomalous cell migration triggers a switch to deviation from the undifferentiated state in colonies of human induced pluripotent stems on feeder layers

Eri Shuzui, Mee-Hae Kim, and Masahiro Kino-oka*

Department of Biotechnology, Graduate School of Engineering, Osaka University, 2-1 Yamadaoka, Suita, Osaka 565-0871, Japan

Received 20 April 2018; accepted 24 July 2018
Available online 14 September 2018

Understanding the fundamental mechanisms that trigger deviation from the undifferentiated state of human induced pluripotent stem cells (hiPSCs) provides key strategies to maintain their undifferentiated state during cell expansion. We assessed deviation from the undifferentiated state in hiPSC colonies by measuring cell migration rates in colonies with deviation that were targeted by the end of culture, in a backward manner. Analyses of migration rates of single cells in colonies with deviation demonstrated that the distribution of migration rates at the region with occurrence of deviated cells had a broad or narrow range compared with those at the regions of undifferentiated cells. It was found that deviated cells in hiPSC colonies accidentally occurred consequent to the appearance of relatively fast or slow migrating cells at the peripheral or central region of colonies, reflecting disorders owing to cell migration anomalies in the hiPSC colony. Fluorescence microscopy for F-actin, paxillin, and E-cadherin clarified the localization of integrin-mediated and cadherin-mediated adhesions, introducing the concept that the occurrence and pattern of deviation in a colony were responsive to changes of cell migration in that colony. Furthermore, a major component of the nuclear lamina, laminA/C displayed a rim at the nuclear periphery in the regions with occurrence of deviated cells, concomitant with the actin cytoskeleton associated with integrin- and cadherin-mediated cell adhesion. These results showed that an anomaly of cell migration in hiPSC colonies led to the accidental appearance of deviated cells therein through alternation of the nuclear lamina and imbalance between cell–cell and cell-substrate interactions.

[**Key words:** Human induced pluripotent stem cells; Deviation of the undifferentiated state; Spatial heterogeneity; Anomaly of cell migration; laminA/C]

The expansion of pluripotent stem cells including embryonic stem cells and induced pluripotent stem cells (iPSCs) remains a challenging process because cells spontaneously lose self-renewal and pluripotent qualities (1). Typically, human iPSC (hiPSC) colonies grow as a monolayer and sustain an undifferentiated state. Undifferentiated hiPSCs form compact colonies of tightly associated cells via cadherin-mediated cell–cell adhesions, exhibiting a small, cobblestone-like morphology (2,3). Upon serial subculture, hiPSCs undergo spontaneous deviation from the undifferentiated state, constituting a well-known phenomenon accompanied by dramatic changes in morphology to large flattened cells at the central or peripheral regions of the colonies (4,5). Such deviated cells are characterized not only by loss of pluripotent characteristics but also as being negative for markers of the three germ layers (6). Transition of hiPSCs from the undifferentiated state to the deviated state in colonies has been designated as deviation (5,6). The deviation could deteriorate the quality of the culture and cause difficulty in the long-term maintenance of hiPSC cultures.

Interactions between the adjacent cells and the extracellular matrix (ECM) are critical in changes in cell and colony morphology, as these potentially activate signaling pathways involved in either maintaining the undifferentiated state of hiPSCs or its deviation (7). The functionality of stem cells is tightly regulated by cell behaviors such as cell–cell adhesions and cell-substrate adhesions, with cell migration often playing an important role in this process (1). Similar to keratinocytes, hiPSC colonies display characteristics of a polarized epithelium including E-cadherin-based cell–cell adhesions and integrin-based adhesions to ECM molecules (8–10). Cell-substrate interactions are typically mediated through focal adhesion-based integrin adhesions, whereas cadherin-based adhesions mediate cell–cell junctions (11). Both cadherins and integrins assemble large intracellular multiprotein complexes via their cytoplasmic domains, which carry out diverse functions such as coupling to the cytoskeleton via adapter proteins and regulating cell behavior through modulation of signaling networks. As both cadherin and integrin act as anchor points that link the actin cytoskeleton to the cell membrane, they are subject to myosin-generated forces that spread through the actin cytoskeleton. In turn, the forces can transduce through cell–cell adhesions into the neighboring cells, and then lead to changes in signal pathway. There is robust evidence from studies in cell culture for mechanotransduction at the levels of cell-substrate interaction and cell–cell interaction (12,13). For example, a recent study has demonstrated that the nucleus can respond directly to cell migration during culture, with alterations in both gene regulation and nuclear mechanical properties that are independent of cytoplasmic biochemical and cytoskeletal responses (14). The mechanisms governing

* Corresponding author. Tel.: +81 6 6879 7444; fax: +81 6 6879 4246.
E-mail address: kino-oka@bio.eng.osaka-u.ac.jp (M. Kino-oka).
Much of this work forms the basis of the Ph.D. dissertation of Eri Shuzui.

1389-1723/$ – see front matter
https://doi.org/10.1016/j.jbiosc.2018.07.020

such complex spatiotemporal mechano-responses, however, have yet to be fully characterized.

In this study, spatial analysis for assessing migration rate was conducted to clarify the trigger for deviation of the cells in the hiPSC colony from the aspect of cell behaviors. Time-lapse observation was performed by retrospective analysis of hiPSC colonies with deviation at the central or peripheral regions. The findings obtained from examining migration rate will allow a better understanding of fundamental mechanisms of cell–cell and cell-substrate interactions from the aspect of triggering deviation from the undifferentiated state of hiPSCs.

MATERIALS AND METHODS

Cells and culture conditions Human iPSCs (hiPSCs) were obtained from the Japanese Collection of Research Bioresources (clone Tic, JCRB Number: JCRB1331). Routine subcultures of hiPSCs were conducted in a culture dish (surface area; 55 cm^2, Corning Costar, Cambridge, MA, USA) using ReproStem medium (ReproCELL Inc., Tokyo, Japan) containing 5 ng/ml basic fibroblast growth factor on a feeder layer of mitomycin C-treated SNL76/7 cells (European Collection of Cell Cultures, Salisbury, UK) or mouse embryonic fibroblasts (MEFs) (ReproCELL Inc.) at 37°C under a 5% CO_2 atmosphere.

For preparation of feeder layers for culturing hiPSCs, feeder cells were seeded at the density of 2.5×10^4 cells/cm^2 on the 0.1% gelatin-coated surfaces and cultivated for one day in Dulbecco's modified Eagle's medium (Sigma–Aldrich, St. Louis, MO, USA) supplemented with 7% fetal bovine serum (FBS; Thermo Fisher Scientific, Waltham, MA, USA) as described previously (5). For passages of hiPSCs, feeder cells were removed after a 1-min incubation with dissociation solution consisting of 0.1 mg/ml collagenase IV, 0.25% trypsin, 20% KSR (all obtained from Thermo Fisher Scientific), and 0.1 mM $CaCl_2$ (Nacalai Tesque, Kyoto, Japan). The hiPSC colonies in the undifferentiated state were carefully collected using a cell scraper (Sumitomo Bakelite Co., Ltd., Osaka, Japan). The suspension of collected undifferentiated colonies was pipetted gently for dispersal into small aggregates, and then dispensed into a fresh culture vessel containing feeder cells. The medium was replaced with fresh medium every day.

Addition of Rac1 inhibitor and activator to hiPSC colonies To mediate change of cell migration, we added 50 μM Rac1 inhibitor (NSC23766; Calbiochem, Merck, Darmstadt, Germany) or 15 μM Rac1 activator (HMG-1; Sigma–Aldrich) from day 5 to day 10.

Time-lapse observation of hiPSC colonies during culture Growth of hiPSC colonies was observed by using an image analyzer with a 4× objective lens (Biostudio; Nikon Engineering Co., Kanagawa, Japan) after seeding hiPSCs on feeder layers.

Quantitative analyses of migration rate and colony size The schematic outline in Fig. 1 shows the procedure of quantification of migration rate. To evaluate the migration rate of single cells in hiPSC colonies, cell nuclei were stained with Hoechst33342 (Thermo Fisher Scientific) for 30 min in live cells. After incubation, cells were washed and fresh medium was added. Time-lapse images of cell nuclei were captured every 30 min over 6 h by using an image analyzer with a 10× objective lens (IN Cell Analyzer 2000; GE Healthcare, Buckinghamshire, UK) from 48 h. The colonies were judged to be with or without deviation at 120 h. To ascertain and quantify the correlation between deviation location and migration rate, the time-lapse images from 48 h to 54 h were used for analysis of cell migration rate at the central and peripheral regions of colonies by retrospective observation. An original image (6.9 mm × 6.9 mm, 16 bit, and 1.35×10^6 pixels/mm^2) was obtained by tilling multi-positioned images. Data were obtained from the two regions of interest (ROIs; 150 μm × 150 μm) placed at the central and peripheral regions of the colony. The centroid position of the colony was set by the outer boundary of the colony in the bright field image. For quantification of cell migration rate, the center coordinates (x_i, y_i) of each nucleus in the ROI were determined using image analysis software (ImageJ; National Institutes of Health, Bethesda, MD, USA). The migration rate, V, of single cells was determined from the displacement of positional centroids of nuclei over 6 h.

In this study, migration rate, V, of single cells was obtained from 5 colonies with and without deviation. The average migration rate, V_M, was calculated from migration rates, V, of 150–300 cells within ROIs of 5 hiPSC colonies. For the comparative analysis, the data of measured migration rate are plotted in a box (15). Migration rates were grouped into bins defined by (i) the [25th percentile −1.5 × (75th percentile −25th percentile)]–25th percentile range, (ii) 25th–75th percentile range, (iii) 75th–[75th percentile +1.5 × (75th percentile −25th percentile)] percentile range, and (iv) outliers of migration rates of single cells in the central and peripheral regions of single colonies.

Immunofluorescence staining The procedure used for immunofluorescence staining was similar to that described previously (16). Briefly, cells were

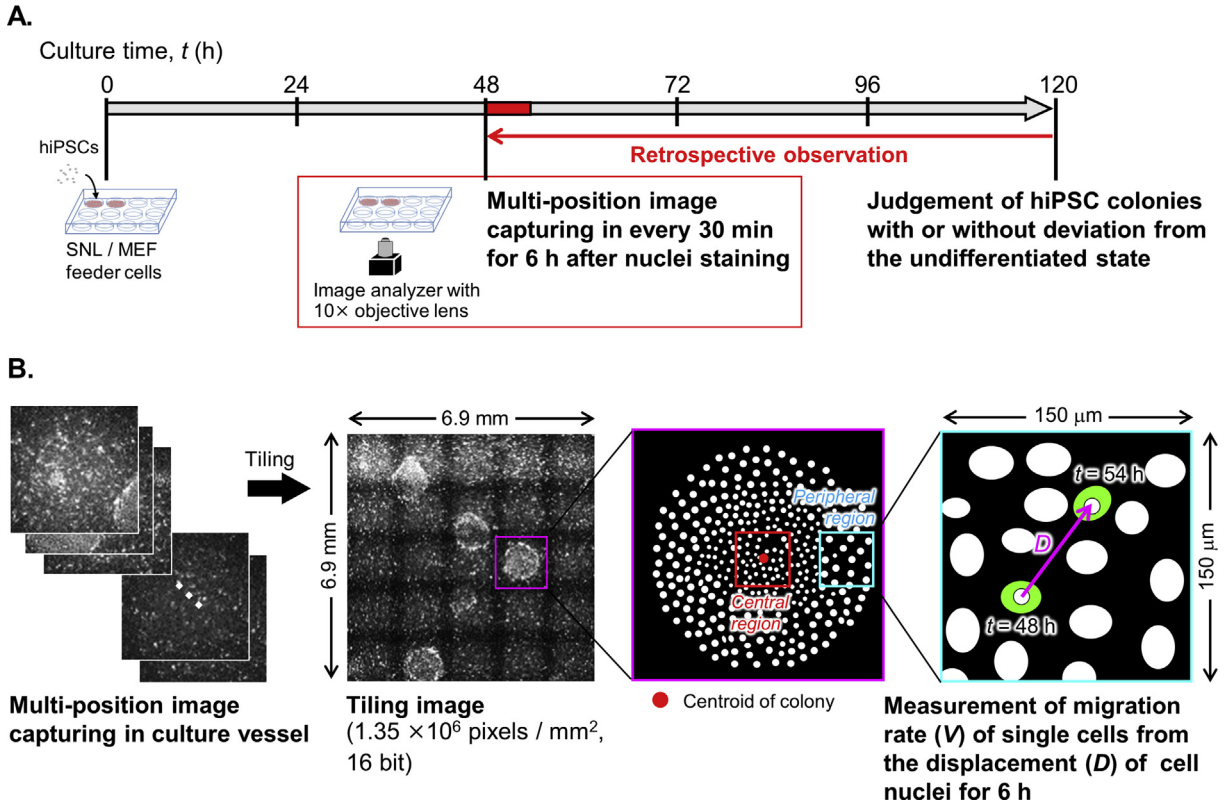

FIG. 1. Procedure of data analyses for the migration rate of the cells at each region of interest (ROI) in hiPSC colonies. (A) Multi-position capturing of bright field and nuclei staining images. (B) Analysis of cell migration rate at the central and peripheral regions of colonies.

washed with phosphate-buffered saline (PBS; Sigma–Aldrich), and fixed with 4% paraformaldehyde (Wako Pure Chemical Industries, Osaka, Japan) for 10 min at room temperature. After washing with PBS, the cells were treated with 0.5% Triton X-100 in PBS for 5 min and rinsed two times in PBS. To mask nonspecific proteins, the cells were incubated in Block Ace (Dainippon Sumitomo Pharma Co. Ltd., Osaka, Japan) for 90 min at room temperature, and treated with a primary antibody at 4°C overnight. The cells were incubated with anti-Oct3/4 (Santa Cruz Biotechnology, Dallas, TX, USA), anti-E-cadherin (Cell Signaling Technology Inc., Beverly, MA, USA), anti-paxillin (Millipore, Billerica, MA, USA), and anti-laminA/C (Santa Cruz Biotechnology) primary antibodies that were adequately diluted in PBS containing 10% Block Ace. After washing with tris-buffered saline, immunolabeling was conducted with Alexa Fluor 488-conjugated goat anti-mouse or Alexa Fluor 594-conjugated anti-rabbit IgG (Thermo Fisher Scientific) for 1 h. F-actin and cell nuclei were stained with Alexa Fluor 594-conjugated phalloidin (Thermo Fisher Scientific) and 4',6-diamidino-2-phenylindole (DAPI; Thermo Fisher Scientific), respectively. The cells were observed using a confocal laser microscope (model FV-1000; Olympus, Tokyo, Japan) through a 60 or 100× objective lens and an image analyzer through a 10× objective lens (IN Cell Analyzer 2000) under fluorescence excitation at 358, 488, and 594 nm.

Statistical analysis The measured hiPSC colonies in each experimental condition were sampled from at least three different cultures. To assess the significance of the differences between undifferentiated colonies and deviated colonies, several statistical tests were used in this study. When data were normally distributed, differences between groups in migration analyses were assessed using the parametric Student's *t*-test. When data were not normally distributed, the nonparametric Mann–Whitney *U*-test was used. The significance threshold was $P < 0.01$.

RESULTS

Characteristics of deviation from the undifferentiated state in colonies of hiPSCs To understand the deviation from the undifferentiated state in colonies of hiPSCs during culture with feeder cells, time-lapse observation was conducted. With elapsed time, the undifferentiated hiPSC colonies grew by a combination of cell division and migration, irrespective of the type of feeder cell (Movie S1). Newly divided cells in colonies basically migrated outward, thereby providing space for newly divided daughter cells across the whole region of the hiPSC colonies. The colonies gradually became larger and more tightly packed, and expanded during culture. As the culture proceeded, the cells at the central region of the growing large colonies in culture with SNL feeder cells protruded, then changed morphologically from small to large flattened cells. The deviated region, evident by changes in the cell morphology, extended sharply, leading to the formation of a colony with a deviated region at the center (Fig. 2A and Movie S1A). In the colonies showing deviation during culture with MEF feeder cells; however, the cells migrated radially away from the edges of the colony. With longer culture, the deviated region proceeded from the periphery, leading to a deviated region at the periphery (Fig. 2B and Movie S1B). Cells deviating from the undifferentiated state were characterized by nuclei lacking Oct3/4 expression (Fig. S1). These findings indicate that the alteration of cell migration in hiPSC colonies is associated with the occurrence of deviation from the undifferentiated state and enlargement of the deviated region.

Supplementary video related to this article can be found at https://doi.org/10.1016/j.jbiosc.2018.07.020.

For investigation of whether changes in cell migration could trigger deviation from the undifferentiated state of hiPSCs, colonies exhibiting deviation in culture with SNL and MEF feeder cells were exposed to a Rac1 activator (HMG1) or inhibitor (NSC23766) to activate or inhibit cell migration, respectively. Incubation with the Rac1 activator or inhibitor-exposed hiPSC colonies with deviation at the central and peripheral regions led to additional occurrence of deviation at the peripheral or central regions, respectively, which are correlated with change of the cell migration in hiPSC colonies (Movie S2 and Fig. S2).

Supplementary video related to this article can be found at https://doi.org/10.1016/j.jbiosc.2018.07.020.

Analysis of migration rates of single cells within and between hiPSC colonies To clarify the correlation between migration rate and deviation of hiPSC colonies, the frequencies of migration rates were evaluated. We compared the distribution of migration rates obtained from the representative hiPSC colonies with deviation in the central or peripheral region by $t = 120$ h. Distributions of migration rates at the central and peripheral regions of colonies with deviation followed a non-normal distribution. Fig. 3 shows the boxplot for distributions of the cell migration rate of single cells in 5 colonies with or without deviation in culture with SNL or MEF feeder cells. In undifferentiated colonies in cultures with SNL and MEF feeder cells by $t = 120$ h, the migration rates of single cells showed a broad distribution in the range of $V = 0.2–12.8$ μm/h and $V = 0.1–13.1$ μm/h, respectively. The distribution of migration rates at the central region had a narrow range compared with those at the peripheral region of the

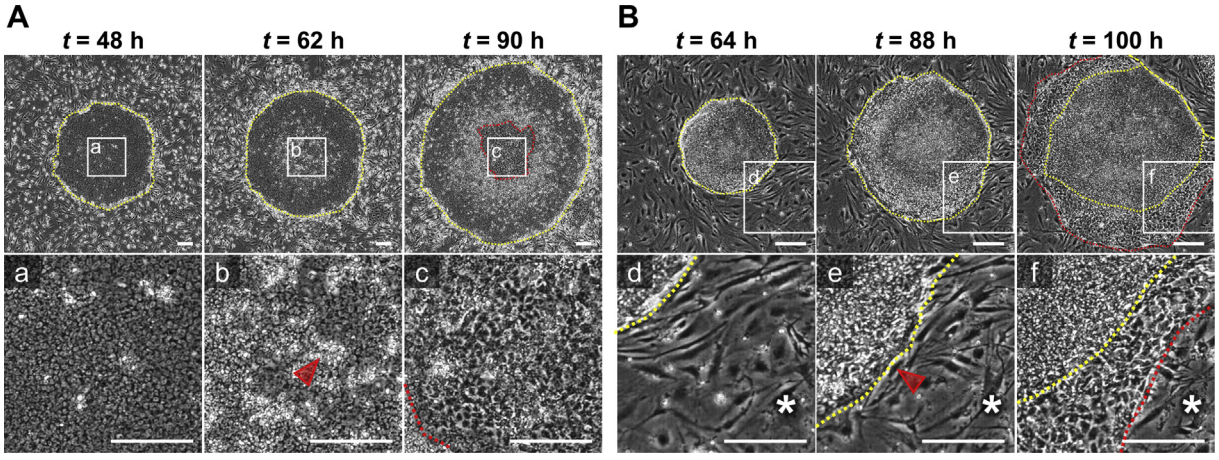

FIG. 2. Occurrence of deviated cells from the undifferentiated state in cultures with SNL (A) and MEF (B) feeder cells. Time-dependent changes of cells in hiPSC colonies are shown. Yellow and red dotted lines indicate the edge of the undifferentiated and deviated regions, respectively. Enlarged panels (a–f) represent cells in the indicated squares of hiPSC colonies. Red arrows show the deviation from the undifferentiated state of hiPSCs. The asterisks show feeder cells. Scale bars: 50 μm. At the central region of colonies in culture with SNL feeder cells, some cells protruded; the region with the deviated cells then enlarged, pushing neighboring cells aside. At the peripheral region of colonies in culture with MEF feeder cells, the region with the deviated cells enlarged outward from the edge of hiPSC colonies. (For interpretation of the references to color in this figure legend, the reader is referred to the Web version of this article.)

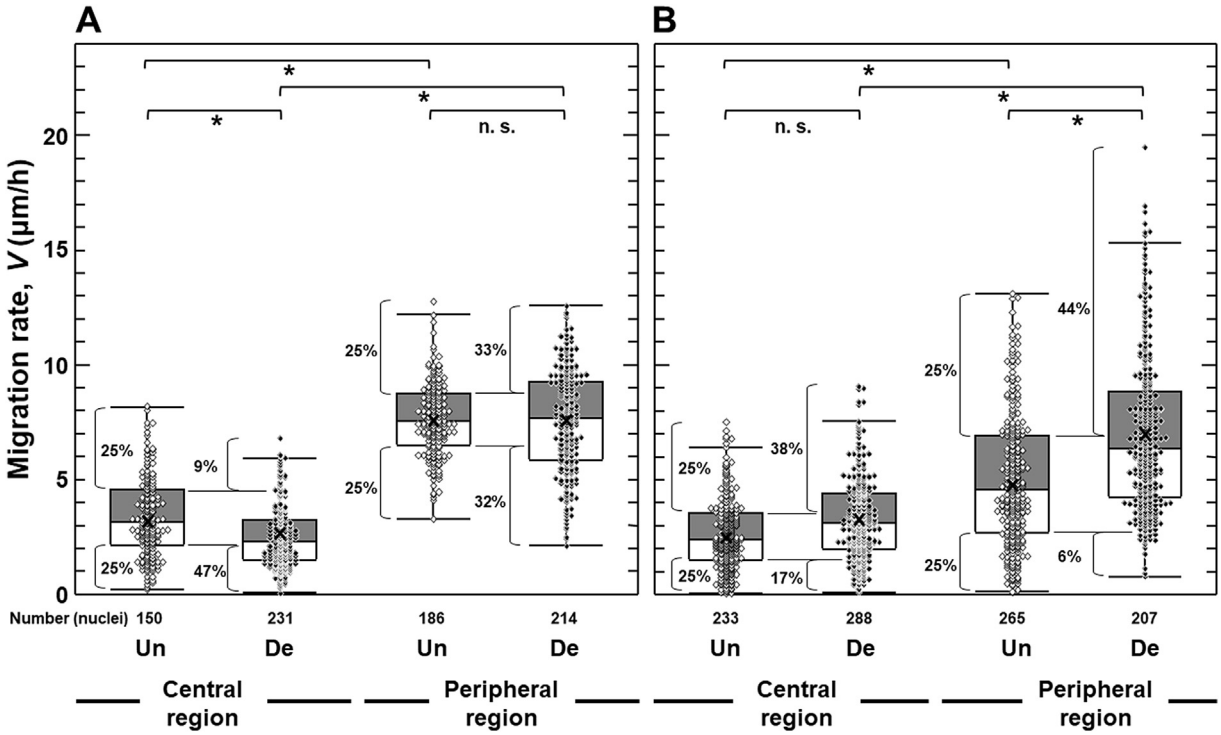

FIG. 3. Distribution of migration rates of single cells at the central and peripheral regions of hiPSC colonies with or without deviation from the undifferentiated state in cultures with SNL (A) and MEF (B) feeder cells. From the retrospective analysis, the data were obtained at $t = 48$ h from five hiPSC colonies. Un indicates hiPSC colonies without deviation by $t = 120$ h. De indicates hiPSC colonies with deviation by $t = 120$ h. Open squares, without deviation; closed squares, with deviation. Cross marks indicate average values. Box-and-whisker plots of migration rates of single cells at the central and peripheral regions of hiPSC colonies. For each box, the central bar is the median, the edges are the 25th and 75th percentiles, and the whiskers extend to the most extreme data points (not including outliers). Outliers are values outside of the range; [25th percentile $-1.5 \times$ (75th percentile $-$25th percentile)] $-$ [75th percentile $+1.5 \times$ (75th percentile $-$25th percentile)]. Data was performed using either Student's t-test or Mann–Whitney U test, accordingly with the results of a test of normality ($^*P < 0.01$).

colony. In both cultures with SNL and MEF feeder cells, the average migration rate, V_M, in the central region was significantly lower than that in the peripheral region of the colony.

In hiPSC colonies with deviation in culture with SNL feeder cells by $t = 120$ h, the migration rates of single cells showed a broad distribution in the range of $V = 0.1$–12.6 μm/h (Fig. 3A). In culture with SNL feeder cells, the average migration rates at the central and peripheral regions were $V_M = 2.7 \pm 1.4$ μm/h and $V_M = 7.6 \pm 2.3$ μm/h, respectively. In comparison, for hiPSC colonies with deviation in culture with MEF feeder cells by $t = 120$ h, the migration rates of single cells showed a broad distribution in the range of $V = 0.1$–19.5 μm/h; these also showed significant difference between central and peripheral regions (Fig. 3B). In hiPSC colonies with deviation at central regions in culture with SNL feeder cells by $t = 120$ h, the ratio of cells with low V values of 0.1–1.5 μm/h increased and the frequency pattern differed from that in culture with MEF feeder cells. In hiPSC colonies with deviation at peripheral regions in culture with MEF feeder cells by $t = 120$ h, however, the ratio of cells with high V values of above 12.6 μm/h increased, although the frequency pattern also differed from that in culture with SNL feeder cells. These findings clearly demonstrated that deviated cells in hiPSC colonies accidentally occurred through the appearance of relatively slow or fast migrating cells at the central or peripheral region of a colony.

In hiPSC colonies with deviation at central regions in culture with SNL feeder cells by $t = 120$ h, the 0–25th percentile range of migration rate was narrow, meaning that the ratio of slow migrating cells increased (Fig. 3A). In hiPSC colonies with deviation at peripheral regions in culture with MEF feeder cells by $t = 120$ h, however, the 75th–100th percentile range of migration rate was wide, meaning that the ratio of fast migrating cells increased (Fig. 3B). In culture with MEF feeder cells, the upper position of the boxplot for the peripheral region of hiPSC colonies reveals that they generally have a larger migration rate in comparison to those in culture with SNL feeder cells. For investigating whether the colonies with deviation exhibit an anomaly of cell migration, thresholds were used from the basis of normality; that is, hiPSC colonies without deviation. The lines for the thresholds were determined at both sides of the distribution in colonies without deviation: 25th and 75th percentile values. At the center of hiPSC colonies with deviation in culture with SNL feeder cells, the ratio below the 25th percentile value was 1.9-fold higher than that in hiPSC colonies without deviation (Fig. 3A). At the periphery of hiPSC colonies with deviation in culture with MEF feeder cells, the ratio above the 75th percentile value was 1.8-fold higher than that in hiPSC colonies without deviation (Fig. 3B). Statistical analysis confirmed that anomaly existed in the hiPSC colonies with deviation. There was statistically significant difference in the distribution shift of median cell migrations between central and peripheral regions, and between SNL and MEF feeder cells.

For the comprehensive analysis, the data in Fig. 3 were replotted in a box plot, which is a graphical representation of the data distribution of migration rates of hiPSC colonies with different colony sizes. When we boxplotted migration rates of single cells against colony size of the initiated cells at $t = 48$ h, we again found a relationship between colony size and the migration rate of single cells (Fig. S3). The distribution of cells at the peripheral region of the colonies with the undifferentiated cells in cultures with SNL and MEF feeder cells by $t = 120$ h revealed that the median value of migration rate exhibited increases with increasing colony sizes

under all culture conditions. For hiPSC colonies with deviation in culture with SNL feeder cells by $t = 120$ h, the median values of migration rate in the central region appeared to have decreased in comparison with the median values in the central region of undifferentiated hiPSC colonies (Fig. S3A). However, the median values at the peripheral region of hiPSCs colonies with deviation in culture with MEF feeder cells was incrementally increased, resulting in a median migration rate range between $V = 4.9 \pm 1.9$ μm/h for 0.21 mm^2 and $V = 11.6 \pm 3.5$ μm/h for 0.80 mm^2 (Fig. S3B). In cultures with SNL or MEF feeder cells, migration measurement at the central or peripheral regions of colonies with deviation, respectively, showed generally smaller or larger values. Specifically, the 0–25th percentile range at the central region of colonies with deviation was smaller than the 75th–100th percentile range in culture with SNL feeder cells (Fig. S3A). In contrast, for culture on MEF feeder cells, the 75th–100th percentile range for cells at the peripheral region of colonies with deviation was larger than 0–25th percentile range (Fig. S3B). Notably, the range of the distribution increased gradually with the increment of colony size. In particular, there were outliers in the measurements for cell migration rate at the peripheral regions of colonies in culture with MEF feeder cells, suggesting that a greater number of anomalous migrating cells had a tendency to achieve a higher rate.

Localization of E-cadherin and paxillin in hiPSC colonies To clarify the mechanism of the occurrence of deviated cells from the undifferentiated state in cultures with SNL and MEF feeder cells, immunostaining for a cell–cell adhesion-associated protein, E-cadherin, and a cell-substrate adhesion-associated protein, paxillin, was performed at $t = 72$ h. The spatial images of F-actin and nuclei indicated that actin stress fibers were abundant along the apical and basal sides of the undifferentiated cells at the peripheral or central regions of the colonies in culture with SNL or MEF feeder cells (Fig. 4). The intact structure of undifferentiated cells was maintained by the integrity of the apical-basal polarity. However, notable differences were observed in the distribution of F-actin and nuclei at the peripheral or central regions of the colonies depending on the feeder type. Comparison of the central and peripheral regions in single colonies revealed a reduction in basal-side actin fibers in the cells located at the central region of the colonies in culture with SNL feeder cells (Fig. 4Db, Eb). Cell nuclei at the central region were partially overlapped and detached from the substrate. In contrast, actin-bundle formation was observed in the cells at the central and peripheral regions of the colonies in culture with MEF feeder cells (Fig. 4Kb, Lb).

Subsequently, the results of immunostaining of E-cadherin and paxillin showed notable differences in their expression that were dependent on location. E-cadherin expression markedly differed in cells between the central and peripheral regions of colonies. Comparison of the central and peripheral regions in single colonies revealed that aberrant expression of E-cadherin appeared at the central regions of the colonies in culture with SNL feeder cells (Fig. 4Ba, Ca). In contrast, E-cadherin was weakly and discontinuously expressed at the peripheral regions of the colonies in culture with MEF feeder cells (Fig. 4Ia, Ja). In cells at the peripheral regions of colonies in culture with SNL and MEF feeder cells, many of the spots of paxillin, a focal adhesion protein, were distributed throughout the cytoplasm and colocalized with F-actin at stress-fiber ends (Fig. 5Gb, Nb). The formation of contractile stress fibers became pronounced, with paxillin indiscriminately distributed throughout the cells. In particular, cells at the peripheral region of colonies in culture with MEF feeder cells showed a leading edge with lamellipodia and strong paxillin spots at the basal side, indicating that the nuclei of the edge cells were subjected to more contractile stress (Fig. 5Nb).

Localization of laminA/C in hiPSC colonies We next investigated whether the nuclei were decorated with laminA/C, as an indicator of a major structural components of the peripheral lamina. Cells at the central region of colonies in culture with SNL feeder cells were smaller and more densely packed than those at the peripheral region, whereas cells at the peripheral region of colonies in culture with MEF feeder cells had much more flattened nuclei than those at the central region (Fig. 6). Immunostaining showed localization of laminA/C at the nuclear periphery of cells located at the central and peripheral regions of colonies in culture with SNL and MEF feeder cells, respectively. In particular, many cells with nuclear peripheral laminA/C were located at the peripheral regions of colonies in culture with MEF feeder cells (Fig. 6D). From the enlarged images, laminA/C displayed a continuous rim at the nuclear periphery of a multilayered cellular structure at the central region in culture with SNL feeder cells, and at the nuclear periphery of large and flattened cells at the peripheral region of colonies in culture with MEF feeder cells (Fig. 6Bb, Fb). These findings indicate that the regions of non-aligned cells in colonies contain nuclear accumulation of laminA/C, likely leading to the deviation from the undifferentiated state of hiPSCs.

DISCUSSION

A mechanism that triggers deviation from the undifferentiated state of hiPSCs in culture Although many studies have focused on the fundamental mechanisms that triggers differentiation of hiPSCs, the deviation trigger from the undifferentiated state during hiPSC culture has been relatively unexplored. In this study, we found that the difference between two types of colonies with deviation during hiPSC culture occurred in cell migratory capacities in response to two types of feeder cells in the culture environment. In culture with SNL feeder cells, motility decreased steadily with increasing population density at the center of colonies with deviation, and the cells overlapped, indicating that cells at the central region of the colony with deviation partially detached from the substrate (Movie S1A). These cells in the central region of large growing colonies with deviation exhibited morphological changes and proliferated while undergoing transition from small cells to large and flattened cells. Conversely, deviation from the undifferentiated state in colonies cultured with MEF feeder cells involved rapidly proliferating and outwardly migrating cells at the periphery of the colony. These cells underwent rapid division in subsequent cultures (Movie S1B). It is most likely that the enhanced migration of hiPSCs in response to MEF feeder cells reduces cell–cell interactions at the peripheral region of colonies and promotes the acquisition of a more motile phenotype. Retrospective analyses of migration rates in colonies with deviation indicated the occurrence of anomalous migration as compared with that at the regions of undifferentiated cells (Fig. 3). The sociological behavior of two populations of relatively fast or slow migrating cells at the peripheral or central regions of colonies with deviation was fundamentally different. These findings provide important information toward understanding the processes of deviation from the undifferentiated state occurring at the center or periphery of hiPSC colonies, suggesting that the balance of interaction between adjacent cells and their substrate along with colony growth is closely related to the occurrence of deviated cells during cell expansion.

Fig. 7 shows a schematic illustration of our working hypothesis based on our observations of deviation from the undifferentiated state of hiPSCs on feeder layers. We hypothesized that (i) anomaly of cell migration in hiPSC colonies leads to imbalance between cell–cell and cell-substrate interactions, and (ii) the accumulation

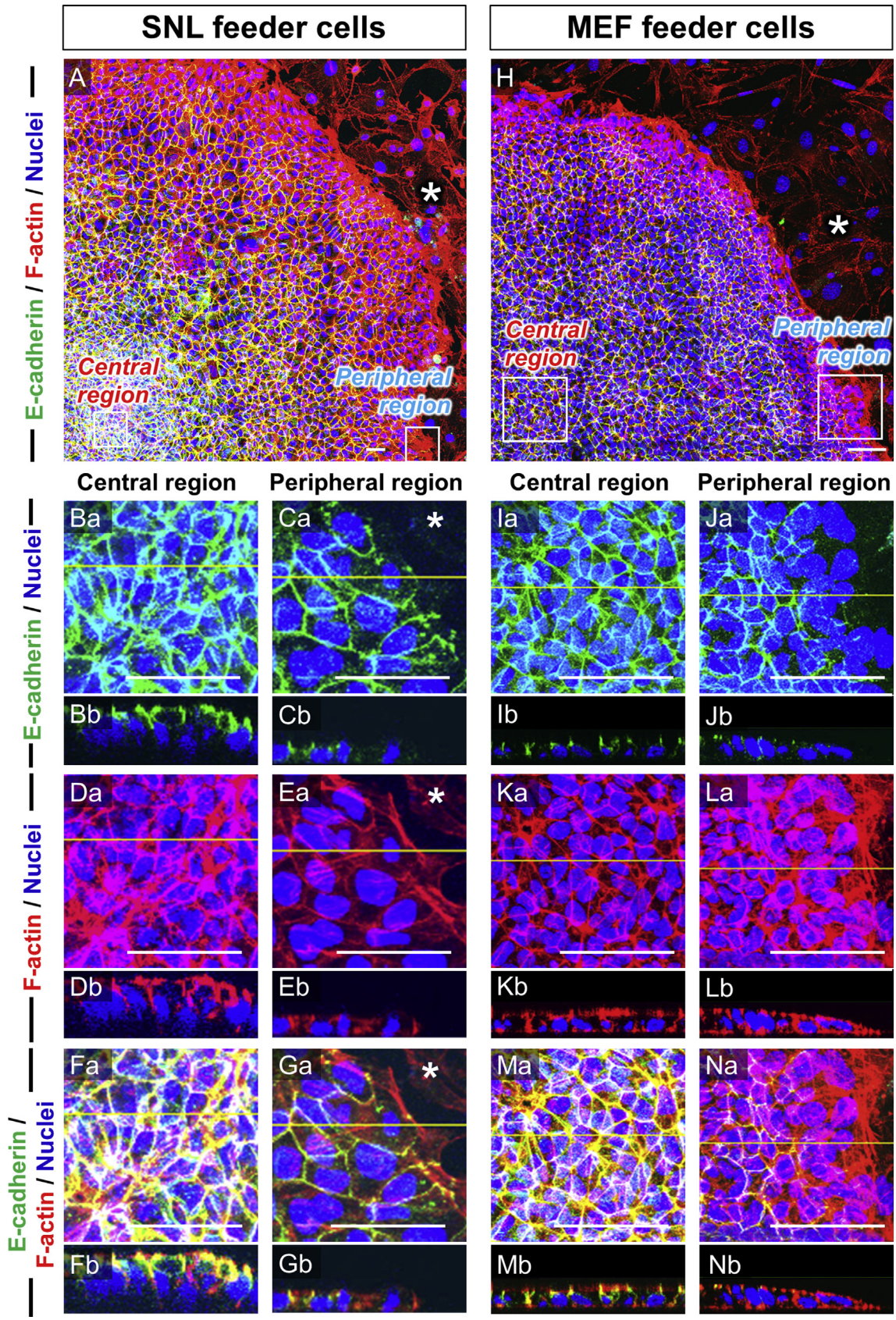

FIG. 4. Localization of E-cadherin associated with actin cytoskeleton in hiPSC colonies in cultures with SNL (A–G) and MEF (H–N) feeder cells at $t = 72$ h. Confocal fluorescence images of E-cadherin (green), F-actin (red), and nuclei (blue) show top-down views of 3D-reconstruction (*XYZ* planes) and 2D optical cross-sectioning (*XZ* planes). Panels are magnified in images of the top-down view (Ba–Ga, Ia–Na) with a cross-sectional side view (Bb–Gb, Ib–Nb). The yellow lines in the top-down views indicate the location of the cross-sectional side view. The asterisks show feeder cells. Scale bars: 40 μm. (For interpretation of the references to color in this figure legend, the reader is referred to the Web version of this article.)

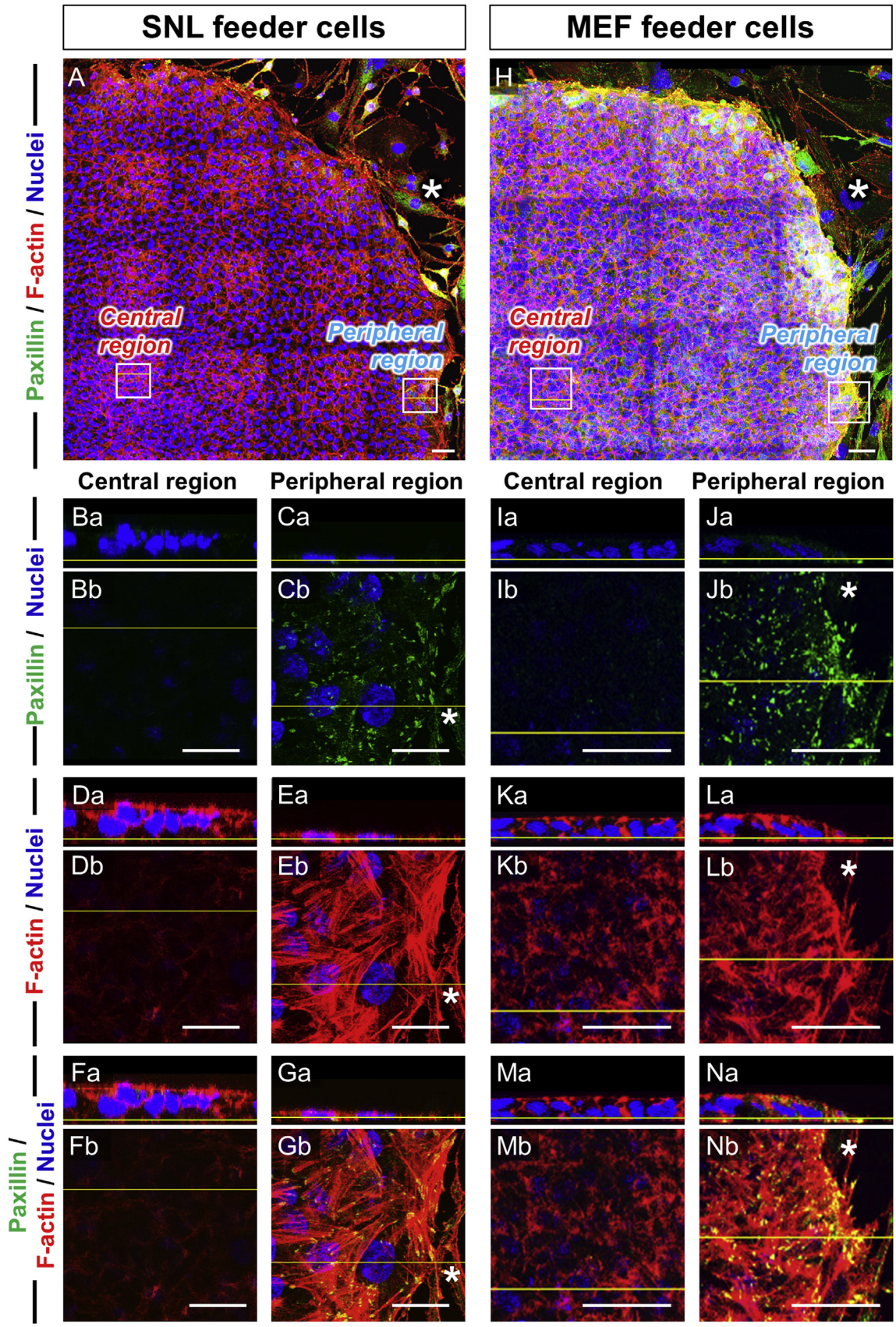

FIG. 5. Focal adhesion formation associated with actin cytoskeleton in hiPSC colonies in cultures with SNL (A–G) and MEF (H–N) feeder cells at $t = 72$ h. Confocal fluorescence images of paxillin (green), F-actin (red), and nuclei (blue) show top-down views of 3D-reconstruction (*XYZ* planes) and 2D optical cross-sectioning (*XY* and *XZ* planes). Panels are magnified in images of a cross-sectional side view in *XZ* (Ba–Ga, Ia–Na) or *XY* planes (Bb–Gb, Ib–Nb). The yellow lines indicate the location of the cross-sectional side view. The asterisks show feeder cells. Scale bars: 40 μm. (For interpretation of the references to color in this figure legend, the reader is referred to the Web version of this article.)

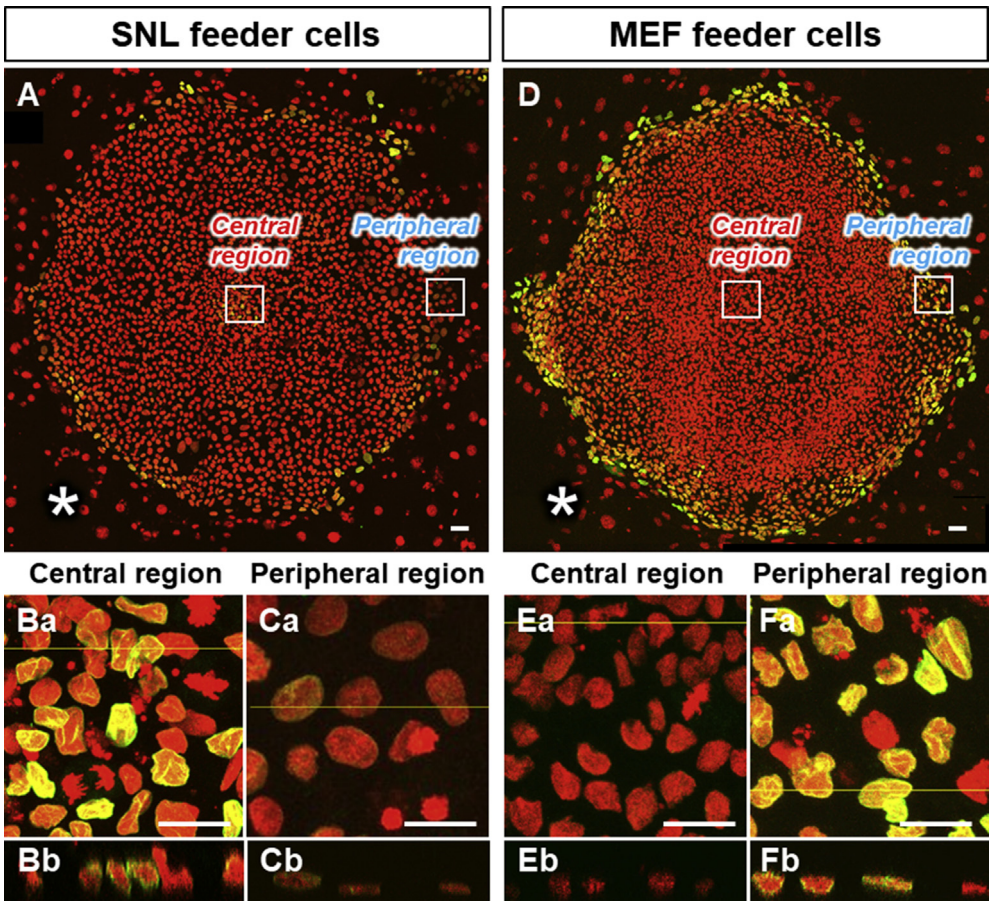

FIG. 6. Localization of laminA/C in hiPSC colonies in cultures with SNL (A–C) and MEF (D–F) feeder cells at $t = 72$ h. Confocal fluorescence images of laminA/C (green) and nuclei (red) show top-down views of 3D-reconstruction (*XYZ* planes) and 2D optical cross-sectioning (*XZ* planes) in hiPSC colonies. Panels are magnified in images of the top-down view (Ba, Ca, Ea, Fa) with a cross-sectional side view (Bb, Cb, Eb, Fb). The yellow lines in top-down views indicate the location of the cross-sectional side view. The asterisks show feeder cells. Scale bars: 20 μm. (For interpretation of the references to color in this figure legend, the reader is referred to the Web version of this article.)

of laminA/C consequent to this imbalance leads to the deviation from the undifferentiated state. This activation leads to conformational change in cadherin and integrin, which are associated with cytoskeleton remodeling. The observed nuclear laminA/C accumulation is consistent with previous findings that nuclear laminA/C expression was absent in pluripotent stem cells and acquired with differentiation (17–19). The transmission of mechanical forces to the nuclear interior and the induced nuclear deformations, which consequently may directly or indirectly modulate gene transcription, depend on the altered migration rate. These changes would be expected to increase stress and/or deformation occurring at sites of nucleus-cytoskeletal linkage and cytoskeletal linkage to the ECM and to the adjacent cell (20). Thus, it appears tempting to speculate that additional nuclear functions may also be regulated as a consequence of actin polymerization in the nucleus, as spreading-mediated nuclear actin dynamics are involved in changes in chromatin organization (12,17,21) and in the control of nuclear shape and positioning such as reported during cell migration. Moreover, as chromatin remodeling constitutes a necessary step in transcription control and its memory, genome integrity, and cellular deformability during migration, our results highlight the importance of cell geometric constraints as critical regulators in cell behavior (22,23). These findings suggest that deviation from the undifferentiated state occurs through the transition to heterochromatin via accumulation of laminA/C at the nuclear periphery through actin cytoskeleton-mediated cell–cell connections and cell-substrate adhesions in the region including associated anomalies of behaviors (24,25).

Studying anomalous cell behaviors as a trigger in fate decision Cell behaviors play a role not only as the trigger for self-renewal mechanisms to be perpetually switched on in stem cell or in cells further down the lineage, but also for the maintenance of diversity of cells. Biologically relevant heterogeneity can be divided into three categories: population heterogeneity, spatial heterogeneity, and temporal heterogeneity (26). Studying the spatio-temporal behavior of cell populations in cultures provides a way to assess alterations in their functions in relation to the mechanisms leading to cell fate decisions in culture. Given the variety of studies and data that have suggested the existence of heterogeneous populations in stem cell cultures, many characteristics can be assessed to reflect different aspects of heterogeneity of cell behaviors (27). For example, the heterogenizing effect of self-renewal and differentiation in culture indicates that the morphology and behavior of single cells are ordered by their topological relationships in colony formation. Because it is difficult to analyze the large amounts of data obtained from cell tracking analyses, there have been few reports using these analyses to identify phenotypes of cells in high cell density cultures (28–31). However, cell-tracking analysis results in detailed data regarding changes in the positions of single cells, providing insight into cell behavior in response to environmental stimuli at different regions in the colony. Cell-to-cell differences in culture are always present to some degree in any population of cells, and the ensemble behaviors of a population may not represent the behaviors of any single cell. The behavior of such cells may be similar to the average behavior of the population, with observed variation being summarized by a mean, and perhaps a variance, with no loss

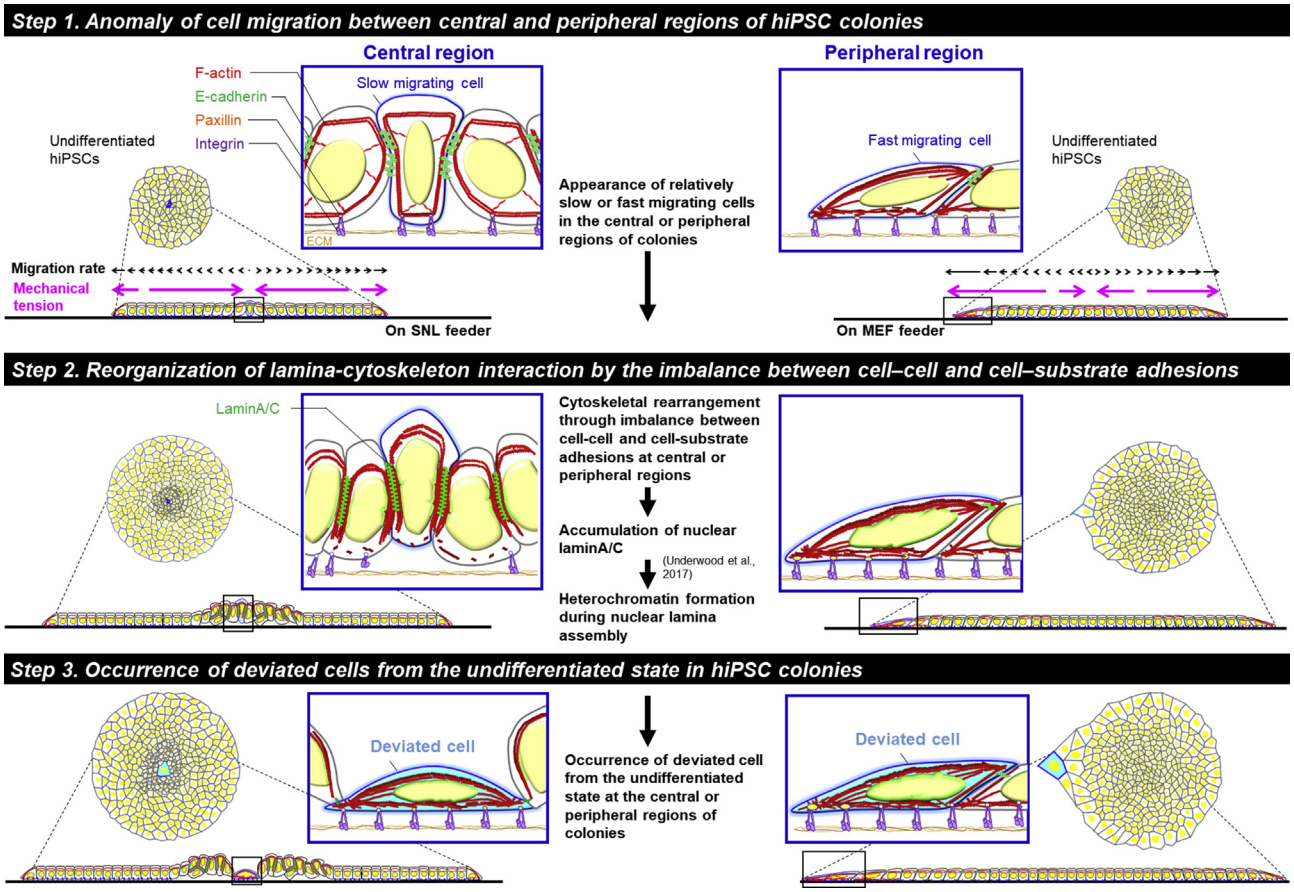

FIG. 7. Schematic drawing of our hypothetical mechanism by which anomalous cell migration acts as a key trigger for deviation from the undifferentiated state of hiPSC colonies in culture with SNL and MEF feeder cells. The nucleus is mechanically linked to the extracellular environment through linker of nucleus and cytoskeleton (LINC) complex connections to a contractile cytoskeleton that interact with the ECM via focal adhesion complexes. When anomalies in cell migration rate occur in hiPSC colonies, the nucleus transforms from a deformable strain sink into a comparatively rigid (relative to the cytoskeleton) stress concentrator, with localization of laminA/C to the nuclear envelope and an increase in heterochromatin content (17). In the undifferentiated state, the nucleus deforms along with the cell, resulting in little added strain (or stress) in the cytoskeleton. This transformation hyper-sensitizes the deviated cell to respond to mechanical perturbation by increasing stress at each point of cytoskeletal connectivity (focal adhesions and LINC complex).

of meaningful biological information. Thus, data from tools and assays that analyze average signals from many cells may not yield the desired result because the cells of interest may be in the minority, i.e., their behavior masked by the majority, or because the dynamics of the populations of interest are offset.

The present study demonstrated that measurement of cell migration served as a valuable tool in understanding the location-dependent changes of single hiPSCs in culture, providing information that may be useful for the development and design of the hiPSC culture process. We focused on an important reason to use nonparametric tests for understanding the deviation trigger from the undifferentiated state during hiPSC culture. Whereas the student's *t*-test constitutes a test of population means, the Mann–Whitney *U*-test is commonly regarded as a test of population medians and interquartile range (32). For cells deviating from the undifferentiated state at the central or peripheral regions of colonies, migration rates are not normally distributed; thus, the Mann–Whitney *U*-test as a non-parametric test is used to compare the two groups for statistical differences. Analysis of migration rate of single cells demonstrated that deviated cells in hiPSC colonies accidentally occurred consequent to the appearance of relatively fast or slow migrating cells (more than 75th or less than 25th percentile values, respectively) at the peripheral or central region of colonies (Fig. 3). From the measurement of single cell migration, we can conclude that deviation from the undifferentiated state of hiPSCs, which are correlated with anomaly of a cell migration in hiPSC colonies. The differences in cell migration might be crucial in determining the point of occurrence for deviated cells from the undifferentiated state. The deviation from the undifferentiated state of hiPSCs was found to accidently occur consequent to anomaly of cell migration, suggesting that the migration rate may constitute a useful parameter to investigate the trigger of deviation in culture. The method introduced here is thus positioned to be useful in assessing the impact of cell behaviors on discrete cellular functions, a possibility that awaits additional study.

In conclusion, we demonstrated that anomalous cell migration triggered hiPSC colonies with deviated cells from the undifferentiated state. We found that such deviation in growing colonies was characterized by morphological changes accompanying an altered migration rate, and accidently occurred in hiPSC colonies. From retrospective analyses of migration rate in colonies with deviation, deviated cells in hiPSC colonies accidentally occurred through the appearance of relatively fast or slow migrating cells at the peripheral or central regions of colonies. In addition, laminA/C accumulation was associated with an imbalance between cell–cell and cell-substrate interactions through anomaly of cell migration, and appeared to serve as a trigger of deviation from the undifferentiated state of hiPSCs. These findings offer important implications for new strategies of culture process design for the expansion of undifferentiated hiPSCs.

Supplementary data related to this article can be found at https://doi.org/10.1016/j.jbiosc.2018.07.020.

ACKNOWLEDGMENTS

This work was supported by the project "Development of cell manufacturing and processing system for industrialization of regenerative medicine" (No. P14006) commissioned by the Japan Agency for Medical Research and Development (AMED).

References

1. **Kim, M. H. and Kino-Oka, M.:** Bioprocessing strategies for pluripotent stem cells based on Waddington's epigenetic landscape, Trends Biotechnol., **36**, 89–104 (2018).
2. **Chen, T., Yuan, D., Wei, B., Jiang, J., Kang, J., Ling, K., Gu, Y., Li, J., Xiao, L., and Pei, G.:** E-cadherin-mediated cell-cell contact is critical for induced pluripotent stem cell generation, Stem Cell, **28**, 1315–1325 (2010).
3. **Redmer, T., Diecke, S., Grigoryan, T., Quiroga-Negreira, A., Birchmeier, W., and Besser, D.:** E-cadherin is crucial for embryonic stem cell pluripotency and can replace OCT4 during somatic cell reprogramming, EMBO Rep., **12**, 720–726 (2011).
4. **Takahashi, K., Narita, M., Yokura, M., Ichisaka, T., and Yamanaka, S.:** Human induced pluripotent stem cells on autologous feeders, PLoS One, **4**, e8067 (2009).
5. **Kim, M. H., Masuda, E., and Kino-oka, M.:** Kinetic analysis of deviation from the undifferentiated state in colonies of human induced pluripotent stem cells on feeder layers, Biotechnol. Bioeng., **111**, 1128–1138 (2014).
6. **Kim, M. H., Sugawara, Y., and Kino-oka, M.:** Botulinum hemagglutinin-mediated selective removal of cells deviating from the undifferentiated state in hiPSC colonies, Sci. Rep., **7**, 93 (2017).
7. **Kim, M. H. and Kino-oka, M.:** Maintenance of an undifferentiated state of human induced pluripotent stem cells through migration-dependent regulation of the balance between cell–cell and cell–substrate interactions, J. Biosci. Bioeng., **119**, 617–622 (2015).
8. **Vaezi, A., Bauer, C., Vasioukhin, V., and Fuchs, E.:** Actin cable dynamics and Rho/Rock orchestrate a polarized cytoskeletal architecture in the early steps of assembling a stratified epithelium, Dev. Cell, **3**, 367–381 (2002).
9. **Delon, I. and Brown, N.:** Integrins and the actin cytoskeleton, Curr. Opin. Cell Biol., **19**, 43–50 (2007).
10. **Kovacs, E. M., Ali, R. G., McCormack, A. J., and Yap, A. S.:** E-cadherin homophilic ligation directly signals through Rac and phosphatidylinositol 3-kinase to regulate adhesive contacts, J. Biol. Chem., **277**, 6708–6718 (2002).
11. **Li, L., Bennett, S. A., and Wang, L.:** Role of E-cadherin and other cell adhesion molecules in survival and differentiation of human pluripotent stem cells, Cell Adh. Migr., **6**, 59–70 (2012).
12. **Thorpe, S. D. and Lee, D. A.:** Dynamic regulation of nuclear architecture and mechanics—a rheostatic role for the nucleus in tailoring cellular mechanosensitivity, Nucleus, **8**, 287–300 (2017).
13. **Rosowski, K. A., Mertz, A. F., Norcross, S., Dufresne, E. R., and Horsley, V.:** Edges of human embryonic stem cell colonies display distinct mechanical properties and differentiation potential, Sci. Rep., **5**, 14218 (2015).
14. **Khatau, S. B., Kusuma, S., Hanjaya-Putra, D., Mali, P., Cheng, L. Z., Lee, J. S., Gerecht, S., and Wirtz, D.:** The differential formation of the LINC-mediated perinuclear actin cap in pluripotent and somatic cells, PLoS One, **7**, e36689 (2012).
15. **Krzywinski, M. and Altman, N.:** Visualizing samples with box plots, Nat. Methods, **11**, 119–120 (2014).
16. **Kim, M. H., Kino-oka, M., Maruyama, N., Saito, A., Sawa, Y., and Taya, M.:** Cardiomyogenic induction of human mesenchymal stem cells by altered Rho family GTPase expression on dendrimer-immobilized surface with D-glucose display, Biomaterials, **31**, 7666–7677 (2010).
17. **Underwood, J. M., Becker, K. A., Stein, G. S., and Nickerson, J. A.:** The ultrastructural signature of human embryonic stem cells, J. Cell. Biochem., **118**, 764–774 (2017).
18. **Heo, S. J., Driscoll, T. P., Thorpe, S. D., Nerurkar, N. L., Baker, B. M., Yang, M. T., Chen, C. S., Lee, D. A., and Mauck, R. L.:** Differentiation alters stem cell nuclear architecture, mechanics, and mechanosensitivity, Elife, **5**, e18207 (2016).
19. **Ihalainen, T. O., Aires, L., Herzog, F. A., Schwartlander, R., Moeller, J., and Vogel, V.:** Differential basal-to-apical accessibility of lamin A/C epitopes in the nuclear lamina regulated by changes in cytoskeletal tension, Nat. Mater., **14**, 1252–1261 (2015).
20. **Wang, N., Tytell, J. D., and Ingber, D. E.:** Mechanotransduction at a distance: mechanically coupling the extracellular matrix with the nucleus, Nat. Rev. Mol. Cell Biol., **10**, 75–82 (2009).
21. **Meshorer, E. and Misteli, T.:** Chromatin in pluripotent embryonic stem cells and differentiation, Nat. Rev. Mol. Cell Biol., **7**, 540–546 (2006).
22. **Guenther, M. G., Frampton, G. M., Soldner, F., Hockemeyer, D., Mitalipova, M., Jaenisch, R., and Young, R. A.:** Chromatin structure and gene expression programs of human embryonic and induced pluripotent stem cells, Cell Stem Cell, **7**, 249–257 (2010).
23. **Akanuma, T., Chen, C., Sato, T., Merks, R. M., and Sato, T. N.:** Memory of cell shape biases stochastic fate decision-making despite mitotic rounding, Nat. Commun., **7**, 11963 (2016).
24. **Francis, R., Xu, X., Park, H., Wei, C. J., Chang, S., Chatterjee, B., and Lo, C.:** Connexin43 modulates cell polarity and directional cell migration by regulating microtubule dynamics, PLoS One, **6**, e26379 (2011).
25. **Versaevel, M., Braquenier, J. B., Riaz, M., Grevesse, T., Lantoine, J., and Gabriele, S.:** Super-resolution microscopy reveals LINC complex recruitment at nuclear indentation sites, Sci. Rep., **4**, 7362 (2014).
26. **Gough, A., Stern, A. M., Maier, J., Lezon, T., Shun, T. Y., Chennubhotla, C., Schurdak, M. E., Haney, S. A., and Taylor, D. L.:** Biologically relevant heterogeneity: metrics and practical insights, SLAS Discov, **22**, 213–237 (2017).
27. **Altschuler, S. J. and Wu, L. F.:** Cellular heterogeneity: do differences make a difference? Cell, **141**, 559–563 (2010).
28. **Lu, M., Xu, B., Jiang, Z., Sheng, A., Zhu, P., and Shi, J.:** Automated tracking approach with ant colonies for different cell population density distribution, Soft Comput., **21**, 3977–3992 (2017).
29. **Dzyubachyk, O., van Cappellen, W. A., Essers, J., Niessen, W. J., and Meijering, E.:** Advanced level-set-based cell tracking in time-lapse fluorescence microscopy, IEEE Trans. Med. Imag., **29**, 852–867 (2010).
30. **Li, K., Miller, E. D., Chen, M., Kanade, T., Weiss, L. E., and Campbell, P. G.:** Cell population tracking and lineage construction with spatiotemporal context, Med. Image Anal., **12**, 546–566 (2008).
31. **Debeir, O., Van Ham, P., Kiss, R., and Decaestecker, C.:** Tracking of migrating cells under phase-contrast video microscopy with combined mean-shift processes, IEEE Trans. Med. Imaging, **24**, 697–711 (2005).
32. **Hart, A.:** Mann-Whitney test is not just a test of medians: differences in spread can be important, BMJ, **323**, 391–393 (2001).